Monomer/Dimer Transition of the Caspase-Recruitment Domain of Human Nod1[†,‡]

Thiagarajan Srimathi,[§,||] Sheila L. Robbins,[§,||] Rachel L. Dubas,[§] Mizuho Hasegawa,[⊥] Naohiro Inohara,[⊥,△] and Young Chul Park*[,§]

Basic Science, Fox Chase Cancer Center, Philadelphia, Pennsylvania 19111, Department of Pathology, University of Michigan Medical School, Ann Arbor, Michigan 48109, and Department of Biochemistry 2nd, Interdisciplinary Graduate School of Medicine and Engineering, University of Yamanashi, 1110 Shimokato, Chuou, Yamanashi 409-3898, Japan

Received August 16, 2007; Revised Manuscript Received November 20, 2007

ABSTRACT: Nod1 is an essential cytoplasmic sensor for bacterial peptidoglycans in the innate immune system. The caspase-recruitment domain of Nod1 (Nod1_CARD) is indispensable for recruiting a downstream kinase, receptor-interacting protein 2 (RIP2), that activates nuclear factor-κB (NF-κB). The crystal structure of human Nod1_CARD at 1.9 Å resolution reveals a novel homodimeric conformation. Our structural and biochemical analysis shows that the homodimerization of Nod1_CARD is achieved by swapping the H6 helices at the carboxy termini and stabilized by forming an interchain disulfide bond between the Cys39 residues of the two monomers in solution and in the crystal. In addition, we present experimental evidence for a pH-sensitive conformational change of Nod1_CARD. Our results suggest that the pH-sensitive monomer/dimer transition is a unique molecular property of Nod1_CARD.

The Nod[1] (nucleotide-binding and oligomerization domain) proteins, in particular Nod1 and Nod2, are essential cytoplasmic sensors for bacterial peptidoglycan derivatives. Nod1 detects *meso*-diaminopimelic acid in Gram-negative and certain Gram-positive bacterial cell walls, while Nod2 acts as a general sensor of bacteria by detecting muramyl dipeptide (*1*−*3*) present in all Gram-positive and Gram-negative bacterial cell walls. It is known that *Nod2* is a susceptibility gene for Crohn's disease (*4*, *5*) and that the polymorphisms in *Nod1* are associated with inflammatory bowel disease (*6*) and asthma (*7*). Moreover, Nod1 is involved in host defense against *Helicobacter pylori* infection of the gastric mucosa, a chronic infection that can lead to peptic ulcers and gastric cancer (*8*).

Nod1 and Nod2 have a common tripartite domain structure—a carboxy-terminal leucine-rich repeat domain (LRR), a centrally located nucleotide-binding and oligomerization domain (NOD), and an amino-terminal caspase-recruitment domain (CARD) (*9*). Nod1 has one CARD, whereas Nod2 has two CARDs. The LRR is involved in ligand recognition (*10*, *11*), and the NOD facilitates self-oligomerization (*12*). The CARDs of Nod1 and Nod2 are indispensable for the recruitment of downstream effectors (*13*−*15*), such as receptor-interacting protein 2 (RIP2, also known as RICK). RIP2 is a CARD-containing serine/threonine kinase that physically associates with Nod1 and Nod2 through CARD−CARD interactions and activates the transcription factor NF-κB. It has also been shown that the oligomerization of Nod1 induces the proximity of RIP2 and that the enforced oligomerization of RIP2 activates NF-κB (*12*).

The CARD is a protein interaction module found in remarkably diverse proteins, which are mainly involved in the activation of caspases and NF-κB (*16*). In general, the CARD participates in multiprotein complex formations where caspases or protein kinases are brought together and activated through the so-called induced proximity mechanism (*17*). To investigate the interactions mediated by the CARD, we purified human Nod1_CARD (residues Met1 to Glu106). The purified Nod1_CARD appeared as a mixture of monomers and dimers. To elucidate the structural aspects of the oligomerization mechanism of Nod1, we solved the crystal structure of homodimeric Nod1_CARD. During the preparation of this manuscript, two NMR structures of monomeric Nod1_CARD (PDB 2B1W and 2DBD; PDB = Protein Data Bank; *18*) and one crystal structure of a homodimeric Nod1_CARD (PDB 2NSN; *19*) were reported. However, the reason for the structural heterogeneity of Nod1_CARD and its functional significance are currently not understood. Here, we present biochemical evidence that homodimeric Nod1_CARD in solution is formed through helix swapping and is stabilized by a subsequent interchain disulfide bond formation, as observed in our crystal structure. In addition, our results indicate that pH-sensitive conformational changes of Nod1_CARD may cause the structural differences between

[†] This work was supported, in part, by the Crohn's and Colitis Foundation of America. Y.C.P. is a Principal Investigator of the Cancer Research Institute.

[‡] The atomic coordinates and structure factors (PDB 2NZ7) have been deposited in the Protein Data Bank, Research Collaboratory for Structural Bioinformatics, Rutgers University, New Brunswick, NJ.

* To whom correspondence should be addressed. Phone: (215) 728-5652. Fax: (215) 728-3574. E-mail: Young.Park@fccc.edu.

[§] Fox Chase Cancer Center.

[||] These authors contributed equally to this work.

[⊥] University of Michigan Medical School.

[△] University of Yamanashi.

[1] Abbreviations: βME, β-mercaptoethanol; DTT, dithiothreitol; iE-DAP, D-glutamyl-*meso*-diaminopimelic acid; IPTG, isopropyl thiogalactoside; MES, 2-(*N*-morpholino)ethanesulfonic acid; NF-κB, nuclear factor-κB; Nod1, nucleotide-binding and oligomerization domain protein 1; Nod1_CARD, caspase-recruitment domain of Nod1; PDB, Protein Data Bank; RIP2, receptor-interacting protein 2; RMSD, root mean square deviation; SDS−PAGE, sodium dodecyl sulfate−polyacrylamide gel electrophoresis.

10.1021/bi7016602 CCC: $40.75
Published on Web 01/11/2008

the NMR structures (PDB 2B1W and 2DBD) and the crystal structures (PDB 2NSN and the structure presented here).

EXPERIMENTAL PROCEDURES

Protein Expression and Purification. The DNA fragments of human Nod1, encoding residues Met1 to Glu106 (Nod1_CARD) and residues Met1 to Asp95 (short_CARD), were inserted into pET24d vector (Novagen) and TOPO100D vector (Invitrogen), respectively, following instructions from the manufacturer. Mutant Nod1_CARDs were generated with the QuikChange II kit (Stratagene), using the plasmid containing Nod1_CARD as a template. The sequences of cloned DNAs were confirmed using DNA sequencers (Applied Biosystems) in the DNA Sequencing Facility at Fox Chase Cancer Center. The oligonucleotide primers used for cloning were made by the DNA Synthesis Facility at Fox Chase Cancer Center. Nod1_CARD and its mutants were expressed and purified as described previously (*20*). Briefly, protein expression was induced in *Escherichia coli* Rosetta-pLysS cells (Novagen) in LB medium supplemented with 0.5% (w/v) glucose by adding 1 mM IPTG at 37 °C for 3 h. Harvested cells were resuspended in a lysis buffer consisting of 50 mM sodium phosphate (pH 7.0), 1.5 M NaCl, 1.5 M urea, 10% (v/v) glycerol, and 3 mM βME. Cleared cell extract was incubated with nickel resin (Qiagen) at room temperature for 1 h, and then the resin was washed with a wash buffer consisting of 50 mM sodium phosphate (pH 6.0), 300 mM NaCl, 10% (v/v) glycerol, 20 mM imidazole, and 3 mM βME. The protein was eluted from the resin with an elution buffer consisting of 50 mM sodium phosphate (pH 6.0), 300 mM NaCl, 10% (v/v) glycerol, 300 mM imidazole, and 3 mM βME. The fractions containing Nod1_CARD were combined and further purified through a Superdex 75 size-exclusion column (Amersham Bioscience) in a buffer consisting of 10 mM sodium phosphate (pH 6.0), 130 mM NaCl, and 1 mM DTT. The fractions containing dimeric Nod1_CARD were concentrated using Amicon Ultra 100K centrifugal filter devices (Millipore). The bacterially expressed Nod1_CARD showed two, very closely located bands on SDS−PAGE gels due to proteolysis during expression (see Supporting Information, Figure S1). Before use, the conformational integrity of the purified proteins was confirmed by circular dichroism using an Aviv 62ABS spectrometer in the Spectroscopy Supporting Facility at Fox Chase Cancer Center to ensure the purified Nod1_CARD consisted of six helices as expected.

Crystallization and Data Collection. Nod1_CARD was crystallized as described previously (*20*). Briefly, crystallization drops consisting of 2.0 μL of purified Nod1_CARD (13.0 mg/ mL) in 10 mM sodium phosphate (pH 6.0), 130 mM NaCl, and 1 mM DTT and 2.0 μL of crystallization solution consisting of 20% (w/v) PEG6000, 67 mM MES (pH 6.0), 100 mM diammonium hydrogen citrate, 90 mM NaI, and 1 mM DTT were equilibrated against 0.9 mL of crystallization solution using the sitting-drop vapor-diffusion method. Small crystals appeared within two weeks. To produce diffraction-quality crystals, small crushed crystals were seeded into new drops containing the same crystallization solution and an equal volume of protein. Crystals appeared within two weeks and reached their maximum dimensions within a month. To obtain heavy atom derivative crystals, native crystals were soaked in cryo solution A consisting of 20% (w/v) PEG6000, 67 mM MES (pH 6.0), 100 mM diammonium hydrogen citrate, and 20% (v/v) glycerol for 30 min and then transferred into a heavy atom solution, consisting of 10 mM $KAu(CN)_2$, $KAuBr_4$, or K_2PtBr_4 in cryo solution A. After 1 h of incubation in the heavy atom solution, the crystals were transferred into cryo solution A for 10 min and then into cryo solution B (cryo solution A with 25% (v/v) glycerol) for 3 min before being flash-cooled in liquid nitrogen. All the experiments, including crystallization and preparation of heavy atom derivative crystals, were performed at 4 °C. The diffraction data sets were collected on beamline F-2 at MacCHESS, Ithaca, NY, using X-rays at a wavelength of 0.977 Å. The native and heavy atom derivative data sets were processed using HKL-2000 (*21*).

Structure Determination and Analysis. The experimental phase information was obtained by the multiple isomorphous replacement method using the Phenix package (*22*). The partial model generated from Phenix was completed using Coot (*23*) and refined using Refmac5 (*24*) from the CCP4 suite (*25*). The statistics for data collection and refinement are summarized in Supporting Information Table S1. The root mean square deviations (RMSDs) for the three-dimensional structure comparisons were calculated using the program Superpose, and the various solvent-accessible surface areas were calculated using Areaimol from the CCP4 suite (*25*). The area of interchain interface and the hydrogen bonds were obtained using PISA (*26*). Protein models shown in the figures were prepared using Pymol (DeLano Scientific LLC).

Size-Exclusion Chromatography Experiments. The conformations of Nod1_CARD and its mutants were tested using 200 μL of proteins that were purified through Ni−NTA affinity chromatography and extensively dialyzed at 4 °C in buffers consisting of 10 mM sodium phosphate (pH 6.0) and 130 mM NaCl with either 1 mM DTT or no DTT. Short_CARD has a higher molecular mass than Nod1_CARD, due to about 3 kDa of extra amino acid residues from TOPO100D vector. The conformations of Nod1_CARD at various pHs were tested using 200 μL of the dimeric protein (about 5 mg/mL) that was purified through size-exclusion chromatography at pH 6.0 with a Superdex 75 column (Amersham Pharmacia). The column was pre-equilibrated with the buffers consisting of 130 mM NaCl, 1 mM DTT, and 10 mM sodium phosphate (pH 6.0), 10 mM Tris−HCl (pH 7.0 or 8.0), or 10 mM sodium acetate (pH 5.0).

Fluorescence Spectroscopy. All fluorescence measurements were performed at 25 °C using a Quantum Master 2000 fluorometer (PTI) in the Spectroscopic Facility at Fox Chase Cancer Center. Homodimeric Nod1_CARD was purified through size-exclusion chromatography using a Superdex 75 column (Amersham Pharmacia) in a buffer consisting of 10 mM sodium acetate (pH 5.0), 130 mM NaCl, and 1 mM DTT. The purified proteins were concentrated to 4 mg/mL and then diluted to 400 μg/mL using buffers consisting of 150 mM NaCl, 1 mM DTT, and 30 mM sodium phosphate (pH 6.0), 30 mM Tris−HCl (pH 7.0 or 8.0), or 30 mM sodium acetate (pH 5.0). The diluted protein samples were dialyzed against the buffers used for the dilution at 4 °C for 3 h. Emission fluorescence of Nod1_CARD, from 300 to 400 nm, was recorded using excitation wavelengths at 280 and 295 nm. To measure the fluorescence of the

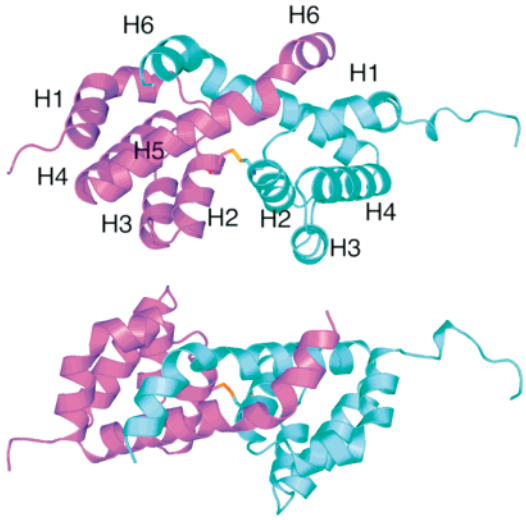

FIGURE 1: Overall structure of homodimeric Nod1_CARD. On the top is the cartoon representation of homodimeric Nod1_CARD. At the bottom the Nod1_CARD is rotated by 90° about the horizontal axis. One monomer (residues Glu8 to Glu106) is colored cyan, and the other monomer (residue Ser14 to Glu106) is colored magenta. The disulfide bond is shown in stick representation.

homodimeric Nod1_CARD with a disulfide bond at various pHs, the proteins were prepared as described above, but without DTT. The secondary structure contents were monitored by circular dichroism using an Aviv 62ABS spectrometer in the Spectroscopy Supporting Facility at Fox Chase Cancer Center.

SDS−PAGE Analysis. The existence of the interchain disulfide bond was examined after mixing with 2× SDS sample buffer (BioRad), supplemented either with 715 mM βME for a reducing condition or without βME for a nonreducing condition. The protein species were separated on a NuPAGE SDS−PAGE gel (Invitrogen) after a 1 min incubation in a boiling water bath.

RESULTS

Overall Structure of Nod1_CARD. The crystal structure of homodimeric Nod1_CARD was determined at 1.9 Å resolution using the multiple isomorphous replacement method (see Supporting Information Table S1). The electron density map unambiguously shows two chains in one asymmetric unit; one extends from Ser14 to Glu106 and the other from Glu8 to Glu106. The structure of Nod1_CARD reveals that the H6 helix (residues Ala96 to Glu106) is swapped with the adjacent monomer to form a homodimeric conformation (Figure 1). In the structure, the H6 helix of one monomer has swung out and bound itself between the H1 and H5 helices of the other monomer. The hinge loop (Asp95 to Asp99) between the H5 and H6 helices of one monomer and the H1−H2 loop (His33 to Thr37) that connects the H1 and H2 helices of the other monomer interact through hydrogen bonds and salt bridges (Supporting Information Table S2). The electron density map also reveals an interchain disulfide bond between the Cys39 of one monomer and the Cys39 of the other monomer (Figure 2). The existence of an interchain disulfide bond in the Nod1_CARD crystals used for X-ray diffraction data collections was confirmed with SDS−PAGE analysis in a nonreducing condition (Supporting Information Figure S1). The residues

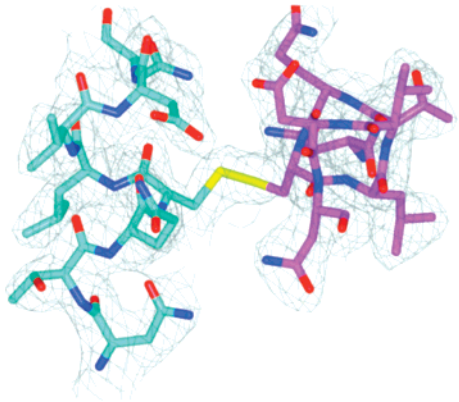

FIGURE 2: $2F_o - F_c$ electron density map for the interchain disulfide bond. The electron density map (gray) shows the disulfide bond that connects Cys39 residues between the two monomers. Residues around Cys39 (Asn36 to Asn43 of each monomer) are shown as sticks colored by atom type (carbon, cyan; each monomer, magenta; nitrogen, blue; oxygen, red; sulfur, yellow).

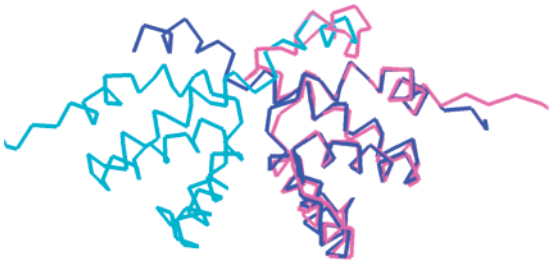

FIGURE 3: Three-dimensional structure alignment of monomeric and homodimeric Nod1_CARDs. The dimeric crystal structure and monomeric NMR structure are superimposed using the program Superpose in the CCP4 suite (*25*). Ribbon representation of homodimeric Nod1_CARD with subunits colored blue and cyan. The NMR structure of monomeric Nod1_CARD (PDB 2DBD) is colored pink.

from Pro18 to Asp95 (H1 to H5 helix) adopt a compact globular fold well-packed around a central hydrophobic core. Four helices, from H2 to H5, form an antiparallel four-helix bundle, and the H1 helix is bent over to cover the hydrophobic core. In addition, the hydrophobic residues of the swapped H6 helix (Leu100, Trp103, and Leu104) participate in covering the remaining exposed surface of the hydrophobic core. The formation of the Nod1_CARD homodimer buries a total of 3145 Å^2 solvent-accessible surface area, 1582 Å^2 from one monomer and 1563 Å^2 from the other monomer. About 87% of this total interface area is provided by the swapping of the H6 helices.

Comparison with Other CARD Structures. To investigate the conformational changes caused by homodimerization, our homodimeric crystal structure of Nod1-CARD was compared to the two recently reported monomeric NMR structures (PDB 2B1W and 2DBD) and the homodimeric crystal structure (PDB 2NSN). The three-dimensional structure alignment shows that our structure is very similar to PDB 2NSN with an RMSD of 0.63 Å. The main difference between these two crystal structures is that our structure has an interchain disulfide bond. Our structure also shows a reasonable RMSD of 1.3 Å from PDB 2DBD (Figure 3). The three-dimensional structure alignment shows that the H6 helix of monomeric Nod1_CARD (PDB 2DBD) is exactly replaced by the swapped H6 helix in our homodimeric structure. The difference between these two structures is that

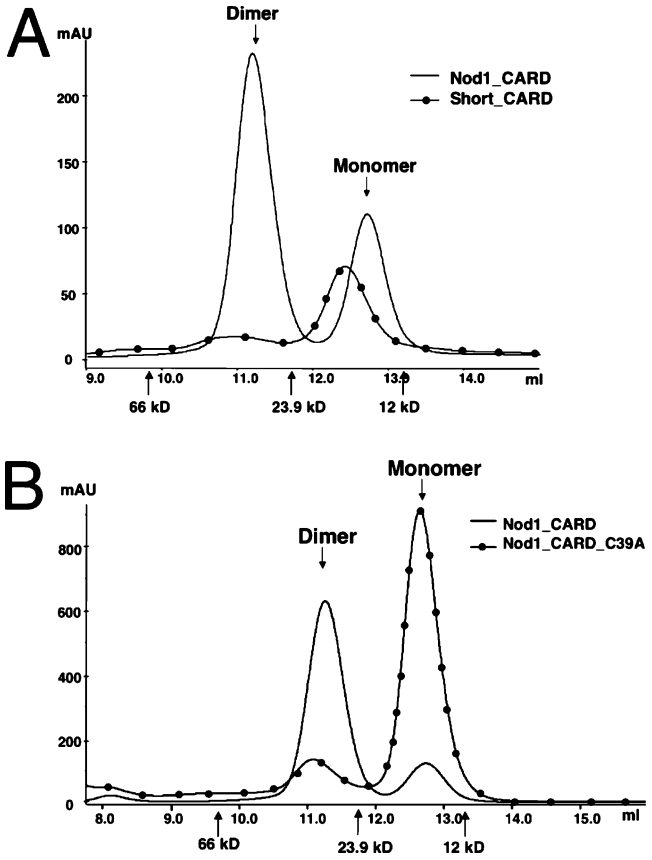

FIGURE 4: (A) Size-exclusion chromatography profiles for Nod1_CARD (about 5 mg/mL) in 1 mM DTT and short_CARD (about 5 mg/mL) in a nonreducing condition. Purified Nod1_CARD and short_CARD were passed through a Superdex 75 column. Short_CARD showed lower optical absorbance due to the lack of Trp residues in the amino acid sequence. (B) Size-exclusion chromatography profiles for Nod1_CARD in 1 mM DTT and Nod1_CARD_C39A in a nonreducing condition. Purified Nod1_CARD (about 15 mg/mL) and Nod1_CARD_C39A (about 15 mg/mL) were passed through a Superdex 75 column.

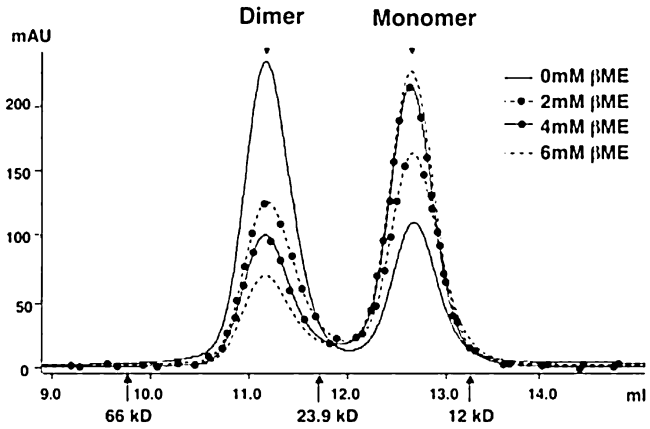

FIGURE 5: Monomer/dimer transition of Nod1_CARD in buffers containing various concentrations of βME. Purified Nod1_CARD (200 μL at 5 mg/mL) was passed through a Superdex 75 size-exclusion column after dialysis in buffers consisting of 10 mM sodium phosphate (pH 6.0), 130 mM NaCl, and 0, 2, 4, or 6 mM βME.

in PDB 2DBD the hinge loop (Asp95 to Asp99) does not interact with the H1−H2 loop (His33 to Thr37). The RMSDs between our structure and PDB 2B1W and between PDB 2DBD and PDB 2B1W are 2.7 Å, which is rather large. In addition, the structure alignment shows that the three-dimensional positions of the amino acid residues in the region between the H2 helix and the H6 helix of PDB 2B1W are inconsistent with PDB 2DBD, PDB 2NSN, and our structure. The overall structure of the homodimeric Nod1_CARD is similar to other CARD structures of Iceberg (PDB 1DGN; *27*) and Apaf-1 (PDB 2YGS and 1CY5; *28*, *29*), with RMSDs of 1.87 and 1.57 Å, respectively.

Role of the H6 Helix in Homodimerization. The structural analysis of Nod1_CARD suggests that the H6 helix plays a key role in homodimerization. To test the role of the H6 helix in the homodimerization of Nod1_CARD, we generated a shorter Nod1_CARD (short_CARD; residues Met1 to Asp95), in which the H6 helix was removed but Cys39 was retained. Size-exclusion chromatography shows that short_CARD is monomeric (Figure 4A). The short_CARD retains its monomeric conformation even at high protein concentrations (up to 5 mg/mL) in the absence of a reducing agent. The crystal structure of Nod1_CARD suggests that the interactions of the hinge region, between the H5 and H6 helices, of one monomer and the loop region that connects the H1 and H2 helices of the other monomer (Supporting Information Table S2) play a role in homodimerization. In addition, the NMR structure of monomeric Nod1_CARD (PDB 2B1W) shows that both the hinge region and loop region are generally exposed to the solvent and do not form significant interactions with other amino acid residues. To understand the importance of the interactions mediated by these regions, we generated mutant Nod1_CARD proteins, in which His33, Arg35, Asn36, Asp95, Tyr97, Asp99, and Arg101 are replaced with Ala. Size-exclusion chromatography of purified mutant Nod1_CARD proteins without a reducing agent shows that the two mutants Nod1_CARD_R35A and Nod1_CARD_D95A are mainly monomeric (Supporting Information Figure S2).

The deletion of the H6 helix (short_CARD) and the mutations, which interrupt the interaction between the hinge and the loop regions, significantly reduce the homodimerization of Nod1_CARD. These results indicate that the H6 helix swapping in Nod1_CARD is a prerequisite for homodimerization and the formation of an interchain disulfide bond. Additionally, it appears that the amino acid residues, Arg35 in the loop region and Asp95 in the hinge region, are involved in the H6 helix swapping of Nod1_CARD.

Role of the Interchain Disulfide Bond in Homodimerization. The homodimeric Nod1_CARD has an interchain disulfide bond in solution and in the crystal (Figure 2B and Supporting Information Figure S1). To evaluate the role of the disulfide bond in the homodimer formation, we generated an Nod1_CARD mutant (Nod1_CARD_C39A), where Cys39 is replaced with Ala. The Nod1_CARD_C39A shows a predominantly monomeric conformation on size-exclusion chromatography under a nonreducing condition (Figure 4B). The importance of the disulfide bond in homodimerization was tested using purified homodimeric Nod1_CARD at various concentrations of βME. This result clearly shows that increasing the concentration of βME results in a proportional increase of the monomeric population of Nod1_CARD (Figure 5). Since the short_CARD remains as a monomer, even in a nonreducing condition (Figure 4A), it appears that the homodimerization process of Nod1_CARD is initiated by H6 helix swapping and the conformation is

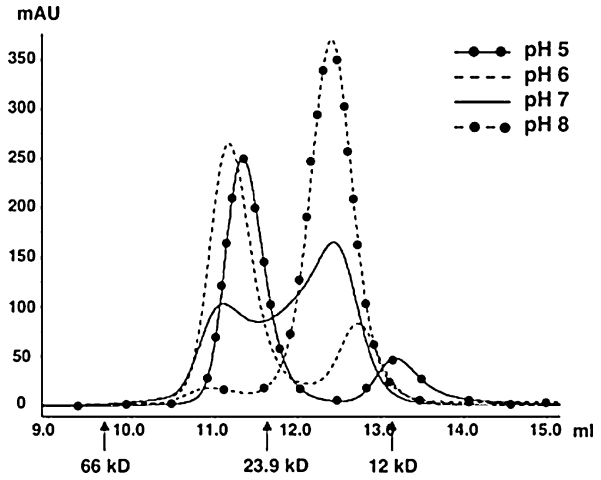

FIGURE 6: Size-exclusion chromatography profiles at various pHs. The purified homodimeric Nod1_CARD (about 5 mg/mL) was passed through a Superdex 75 column at pH 5.0, 6.0, 7.0, and 8.0.

then stabilized by disulfide bond formation between the two Cys39 residues.

Effect of pH on the Quaternary Structure of Nod1_CARD. It is known that the energy barrier between the monomer and the swapped dimer can be reduced by a change in solution conditions (*30*). In our experiments, we observed that Nod1_CARD exists mostly as dimers at pH 6.0 and monomers at pH 7.0. In addition, Nod1_CARD is monomeric at pH 7.0 in NMR structures (*18*), but the crystal structures are homodimeric at pH 6.0 in this paper and at pH 4.7 in PDB 2NSN (*19*). To test the effect of pH on conformation, the purified homodimeric Nod1_CARD at pH 6.0 was passed through a size-exclusion column at various pHs. The result shows that homodimeric Nod1_CARD completely dissociates to monomers at pH 8.0, but remains as dimers at pH 5.0. Nod1_CARD prefers the homodimeric conformation at pH 6.0, but the monomeric conformation at pH 7.0 (Figure 6). The presence of the interchain disulfide bond in the dimer fractions, which were eluted from the size-exclusion column, was confirmed by nonreducing SDS−PAGE analysis (data not shown).

Effects of pH on the Tertiary Structure of Nod1_CARD. Our results show that H6 helix swapping is a prerequisite for the quaternary structural change of Nod1_CARD, which is pH-sensitive. This observation suggests that the tertiary structure of Nod1_CARD might also be sensitive to pH change. Nod1_CARD has one Trp residue, Trp103, located on the H6 helix that is swapped during homodimerization. We examined the pH-dependent tertiary structural change around the H6 helix by monitoring the intrinsic Trp fluorescence changes of Nod1_CARD at various pHs (Figure 7A). The intrinsic Trp fluorescence of Nod1_CARD is the lowest at pH 5.0. At pH 6.0 and 7.0, the Trp fluorescence is increased from the fluorescence at pH 5.0 by about 20% and 25%, respectively. At pH 8.0 the fluorescence increases by about 50% from the fluorescence at pH 5.0. The maximum emission wavelength is not significantly shifted. The subsequent nonreducing SDS−PAGE analysis of the samples confirms that the increasing Trp fluorescence was accompanied by a reduction of the disulfide bond, which correlates with monomerization (Figure 7B). In contrast, the pH change does not affect the secondary structural content of Nod1_CARD since circular dichroism spectra recorded

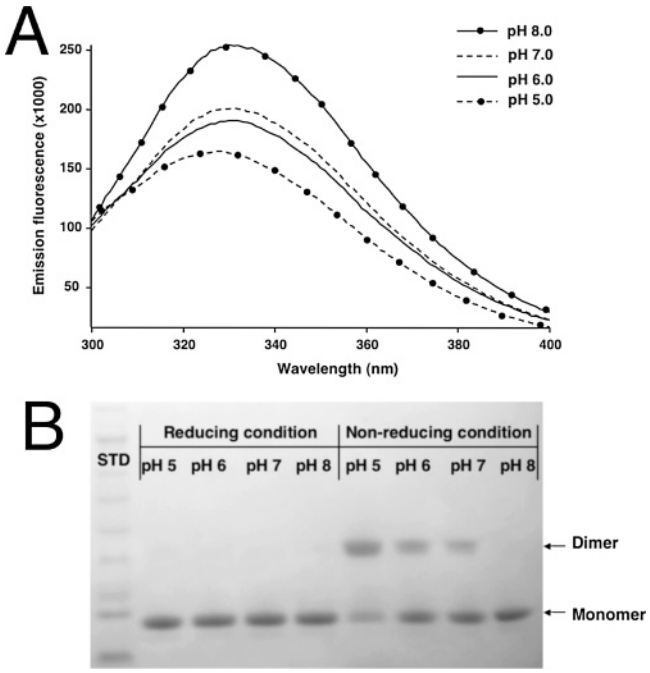

FIGURE 7: pH-dependent conformational change of Nod1_CARD. (A) The emission fluorescence spectra of Nod1_CARD (400 μg/mL) at pH 5.0, 6.0, 7.0, and 8.0 were recorded using an excitation wavelength of 295 nm. (B) The protein samples used for recording fluorescence spectra were analyzed using SDS−PAGE in a reducing condition and a nonreducing condition. The lane marked "STD" is the molecular weight standard.

at various pHs are indistinguishable (Supporting Information Figure S3). To test whether pH can affect the tertiary structure around the H6 helix in a homodimeric Nod1_CARD with a disulfide bond, we monitored the intrinsic Trp fluorescence changes of homodimeric Nod1_CARD at various pHs without a reducing agent. However, the result shows that the Trp fluorescence of homodimeric Nod1_CARD is not affected by pH changes (Supporting Information Figure S4). Our results indicate that the homodimerization of Nod1_CARD in solution is sensitive to pH and accompanies the tertiary structural changes, in particular around the H6 helix, as seen in our crystal structure. The tertiary structure around the H6 helix becomes stable as Nod1_CARD proteins adopt dimers stabilized by a disulfide bond. On the basis of these observations, we propose that differences in pH may explain the conformational heterogeneity of Nod1_CARD observed in the NMR and crystal structures.

DISCUSSION

Four structures of Nod1_CARD, including the one presented here, recently became available in the PDB. Through structural and biochemical experiments, we show that the homodimerization of Nod1_CARD can occur through helix swapping and an interchain disulfide bond formation in both solution and crystals.

Our close investigation found that all of the amino acid residues in PDB 2B1W starting from Asp66 moved exactly three residues back. For example, the three-dimensional position of Leu72 in the H4 helix in our structure is occupied by the same Leu residues in PDB 2NSN and 2DBD, but this position is occupied by Arg69 in PDB 2B1W. Misassignment of residues in the loop between Pro63 and Pro65 of the NMR structure may explain the structural differences

between PDB 2B1W and the other Nod1_CARD structures. The crystal structure of PDB 2NSN was solved by the molecular replacement method using the NMR structure of Iceberg (PDB 1DGN) as a model. However, Nod1_CARD has a conformation and amino sequence quite different from those of Iceberg, which is monomeric and whose sequence identity to Nod1_CARD is only 25.5%. We determined the crystal structure of Nod1_CARD using the multiple isomorphous replacement method to obtain experimental phase information through an extensive search for heavy atom derivative crystals, since the molecular replacement method did not provide a satisfying phase solution. Our biochemical results suggest that the purified Nod1_CARD that was used for the structural determination of PDB 2NSN might exist as mostly monomers or a mixture of monomers and dimers in solution because of the high concentration of reducing agent (5 mM DTT) and the slightly basic pH (8.0) used during purification. Then, the protein might form a dimeric conformation in the crystal because of the high protein concentration and the acidic crystallization condition (pH 4.7). The available structures and the structure reported here may represent sequential steps in Nod1_CARD dimerization. The NMR structures represent the monomeric status of Nod1 at neutral pH. Under this condition, Nod1_CARD has a relatively flexible tertiary structure around the H6 helix. PDB 2NSN may be similar to the intermediate state of the dimerization of Nod1_CARD, in which monomeric Nod1_CARDs are placed in close proximity by the oligomerization of activated Nod1 and H6 helix swapping is induced by the high local protein concentration. This dimeric intermediate conformation of Nod1_CARD is not stable in solution, however. As seen in the crystal structure presented here, the conformation is then stabilized by forming a disulfide bond between the two Cys39 residues that are brought together at a proper angle by the H6 helix swapping.

Three factors that affect free energy differences between the monomers and the domain-swapped oligomers were suggested through analysis of about 40 structurally characterized cases of domain-swapped proteins (*30*). First, greater entropy of the monomer makes it more favored thermodynamically. Second, hinge loops may form new interactions in the domain-swapped dimer, which favor dimerization. Third, new interactions at the open interface make the domain-swapped oligomer more favorable thermodynamically. Our structural and biochemical analyses show that the Nod1_CARD favors the monomeric conformation at neutral and basic pHs as seen in the NMR structures (Figure 6). The hinge loop of Nod1_CARD generates six hydrogen bonds with the H1−H2 loop, when it forms a dimer (Supporting Information Table S2). In addition, interchain disulfide bond formation at the open interface stabilizes the homodimeric conformation of Nod1_CARD (Figure 4B). Therefore, the suggested model of domain swapping (*31*) fits well to the dimerization mechanism of Nod1_CARD. In addition, the pH-sensitive monomer/dimer transition of Nod1_CARD indicates that acidic pH reduces the high-energy barrier between the monomer and the swapped dimer and promotes homodimerization in solution and crystals.

It appears that the conformation of the H6 helix is intrinsically flexible because conformational heterogeneity of the H6 helix was observed during NMR structure determination (*18*) and because monomeric Nod1_CARD can coexist with homodimeric Nod1_CARD in solution. The intrinsic flexibility of the H6 helix of Nod1_CARD may play a role in the formation of the active and stable oligomeric structure of Nod1 in the context of high local concentration of the CARD, which is produced through the self-oligomerizion of NOD when Nod1 is activated by ligand detection (*12*). We tested the physiological significance of the homodimerization of Nod1_CARD using transfected HEK293T cells with plasmids for full-length Nod1 and full-length Nod1 mutants. The Nod1 mutants tested included the Cys39Ser, His33Ala, Asn36Ala, Asp95Ala, and Arg101Glu mutations that disturb the formation of the interchain disulfide bond and the hydrogen bond network between the H1−H2 loop (His33 to Thr37) and the hinge loop (Asp95 to Asp99). Although the mutations of residues Cys39 and Asp95 generate mainly monomeric Nod1_CARD *in vitro* (Figure 5), *in vivo* the Nod1 mutants produced levels of NF-κB activation similar to those of wild-type Nod1, upon treatment with the Nod1-specific ligand γ-D-glutamyl-*meso*-diaminopimelic acid (iE-DAP) (unpublished data). This might be due to the following reasons: (1) Upon detecting its ligand, Nod1 is expected to form an apoptosome-like oligomeric structure to recruit and activate RIP2 (*31*). The oligomerization of Nod1, leading to a high local concentration of CARD, is achieved by the NOD of Nod1, not by CARD. (2) The key amino acid residues of Nod1_CARD, Glu53, Asp54, and Glu56, for Nod1−RIP2 interaction (*18*) are located on the opposite side of the H6 helices, remote from the Cys39 residues that we have shown mediate homodimerization. (3) At the high local concentration of CARD in the apoptosome-like structure, Nod1_CARD can form the domain-swapped intermediate dimer as seen in PDB 2NSN (*19*). Since the physiological significance of Nod1_CARD dimerization is not clear from our *in vivo* tests, we attempted to investigate the *in vitro* interaction between Nod1_CARD and RIP2. However, our recombinant RIP2 proteins were not stable and quickly aggregated or precipitated. Although more biological and biochemical studies are required to understand the functional implications of the monomer/dimer transition of Nod1_CARD in Nod1-induced NF-κB activation, we suggest that the disulfide bond formation in homodimerization might be a stabilization mechanism of activated Nod1, similar to that seen in the structures of caspase-2 (*32*) and prion proteins (*33*).

To date, this is the first report of a CARD that can undergo the pH-sensitive monomer/dimer transitions through helix swapping and interchain disulfide bond formation without major changes to the secondary structure. We propose that this is a unique molecular property of Nod1_CARD. Since there is insufficient accumulated data for the other members of the CARD protein family, direct comparison of this molecular property of Nod1_CARD to those of other CARDs is limited. The three-dimensional structure of the complex between Nod1_CARD and RIP2_CARD, as well as of full-length Nod1, is required to improve our understanding of the Nod1-mediated interactions and their physiological role in the innate immune response.

ACKNOWLEDGMENT

We thank the staff at Macromolecular Diffraction at CHESS (MacCHESS) Facility beamline F-2 and at NSLS beamline X12C for their assistance with data collection.

SUPPORTING INFORMATION AVAILABLE

Figures and tables showing SDS−PAGE analysis of Nod1_CARD in nonreducing and reducing conditions, size-exclusion chromatography for Nod1_CARD_R35A and Nod1_CARD_D95A, far-ultraviolet circular dichroism spectra for purified homodimeric Nod1_CARD at various pHs, pH effect on the Trp fluorescence of dimeric Nod1_CARD, statistics of diffraction data collection and structural refinement of Nod1_CARD, and interactions between two monomers of Nod1_CARD. This material is available free of charge via the Internet at http://pubs.acs.org.

REFERENCES

1. Girardin, S. E., Boneca, I. G., Carneiro, L. A., Antignac, A., Jehanno, M., Viala, J., Tedin, K., Taha, M. K., Labigne, A., Zahringer, U., Coyle, A. J., DiStefano, P. S., Bertin, J., Sansonetti, P. J., and Philpott, D. J. (2003) Nod1 detects a unique muropeptide from gram-negative bacterial peptidoglycan, *Science 300*, 1584−1587.
2. Girardin, S. E., Boneca, I. G., Viala, J., Chamaillard, M., Labigne, A., Thomas, G., Philpott, D. J., and Sansonetti, P. J. (2003) Nod2 is a general sensor of peptidoglycan through muramyl dipeptide (MDP) detection, *J. Biol. Chem. 278*, 8869−8872.
3. Inohara, N., Ogura, Y., Fontalba, A., Gutierrez, O., Pons, F., Crespo, J., Fukase, K., Inamura, S., Kusumoto, S., Hashimoto, M., Foster, S. J., Moran, A. P., Fernandez-Luna, J. L., and Nuñez, G. (2003) Host recognition of bacterial muramyl dipeptide mediated through NOD2. Implications for Crohn's disease, *J. Biol. Chem. 278*, 5509−5512.
4. Hugot, J. P., Chamaillard, M., Zouali, H., Lesage, S., Cezard, J. P., Belaiche, J., Almer, S., Tysk, C., O'Morain, C. A., Gassull, M., Binder, V., Finkel, Y., Cortot, A., Modigliani, R., Laurent-Puig, P., Gower-Rousseau, C., Macry, J., Colombel, J. F., Sahbatou, M., and Thomas, G. (2001) Association of NOD2 leucine-rich repeat variants with susceptibility to Crohn's disease, *Nature 411*, 599−603.
5. Ogura, Y., Bonen, D. K., Inohara, N., Nicolae, D. L., Chen, F. F., Ramos, R., Britton, H., Moran, T., Karaliuskas, R., Duerr, R. H., Achkar, J. P., Brant, S. R., Bayless, T. M., Kirschner, B. S., Hanauer, S. B., Nunez, G., and Cho, J. H. (2001). A frameshift mutation in NOD2 associated with susceptibility to Crohn's disease, *Nature 411*, 603−606.
6. McGovern, D. P., Hysi, P., Ahmad, T., van Heel, D. A., Moffatt, M. F., Carey, A., Cookson, W. O., and Jewell, D. P. (2005) Association between a complex insertion/deletion polymorphism in NOD1 (CARD4) and susceptibility to inflammatory bowel disease, *Hum. Mol. Genet. 14*, 1245−1250.
7. Hysi, P., Kabesch, M., Moffatt, M. F., Schedel, M., Carr, D., Zhang, Y., Boardman, B., von Mutius, E., Weiland, S. K., Leupold, W., Fritzsch, C., Klopp, N., Musk, A. W., James, A., Nunez, G., Inohara, N., and Cookson, W. O. (2005) NOD1 variation, immunoglobulin E and asthma, *Hum. Mol. Genet. 14*, 935−941.
8. Viala, J., Chaput, C., Boneca, I. G., Cardona, A., Girardin, S. E., Moran, A. P., Athman, R., Memet, S., Huerre, M. R., Coyle, A. J., DiStefano, P. S., Sansonetti, P. J., Labigne, A., Bertin, J., Philpott, D. J., and Ferrero, R. L. (2004) Nod1 responds to peptidoglycan delivered by the *Helicobacter pylori* cag pathogenicity island, *Nat. Immunol. 5*, 1166−1174.
9. Inohara, N., and Nunez, G. (2003) NODs: intracellular proteins involved in inflammation and apoptosis, *Nat. Rev. Immunol. 3*, 371−382.
10. Girardin, S. E., Tournebize, R., Mavris, M., Page, A. L., Li, X., Stark, G. R., Bertin, J., DiStefano, P. S., Yaniv, M., Sansonetti, P. J., and Philpott, D. J. (2001) CARD4/Nod1 mediates NF-κB and JNK activation by invasive *Shigella flexneri*, *EMBO Rep. 2*, 736−742.
11. Inohara, N., Ogura, Y., Chen, F. F., Muto, A., and Nunez, G. (2001) Human Nod1 confers responsiveness to bacterial lipopolysaccharides, *J. Biol. Chem. 276*, 2551−2554.
12. Inohara, N., Koseki, T., Lin, J., del Peso, L., Lucas, P. C., Chen, F. F., Ogura, Y., and Nunez, G. (2000) An induced proximity model for NF-kappa B activation in the Nod1/RICK and RIP signaling pathways, *J. Biol. Chem. 275*, 27823−27831.
13. Bertin, J., Nir,. W. J., Fischer, C. M., Tayber, O. V., Errada, P. R., Grant, J. R., Keilty, J. J., Gosselin, M. L., Robison, K. E., Wong, G. H., Glucksmann, M. A., and DiStefano, P. S. (1999) Human CARD4 protein is a novel CED-4/Apaf-1 cell death family member that activates NF-kappaB, *J. Biol. Chem. 274*, 12955−12958.
14. Inohara, N., Koseki, T., del Peso, L., Hu, Y., Yee, C., Chen, S., Carrio, R., Merino, J., Liu, D., Ni, J., and Nunez, G. (1999) Nod1, an Apaf-1-like activator of caspase-9 and nuclear factor-kappaB, *J. Biol. Chem. 274*, 14560−14567.
15. Ogura, Y., Inohara, N., Benito, A., Chen, F. F., Yamaoka, S., and Nunez, G. (2001) Nod2, a Nod1/Apaf-1 family member that is restricted to monocytes and activates NF-kappaB, *J. Biol. Chem. 276*, 4812−4818.
16. Reed, J. C., Doctor, K. S., and Godzik, A. (2004) The domains of apoptosis: a genomics perspective, *Sci. STKE 239*, re9.
17. Boatright, K. M., Renatus, M., Scott, F. L., Sperandio, S., Shin, H., Pedersen, I. M., Ricci, J. E., Edris, W. A., Sutherlin, D. P., Green, D. R., and Salvesen, G. S. (2003) A unified model for apical caspase activation, *Mol. Cell 11*, 529−541.
18. Manon, F., Favier, A., Nunez, G., Simorre, J. P., and Cusack, S. (2007) Solution structure of NOD1 CARD and mutational analysis of its interaction with the CARD of downstream kinase RICK, *J. Mol. Biol. 365*, 160−174.
19. Coussens, N. P., Mowers, J. C., McDonald, C., Nunez, G., and Ramaswamy, S. (2007) Crystal structure of the Nod1 caspase activation and recruitment domain, *Biochem. Biophys. Res. Commun. 353*, 1−5.
20. Srimathi, T., Robbins, S. L., Dubas, R. L., Seo, J. H., and Park, Y. C. (2007) Purification, crystallization and preliminary crystallographic characterization of the caspase-recruitment domain of human Nod1, *Acta Crystallogr., Sect. F: Struct. Biol. Cryst. Commun. 63*, 21−23.
21. Otwinowski, Z., and Minor, W. (1997) Processing of X-ray diffraction data collected in oscillation mode, *Methods Enzymol. 276*, 307−326.
22. Adams, P. D., Grosse-Kunstleve, R. W., Hung, L. W., Ioerger, T. R., McCoy, A. J., Moriarty, N. W., Read, R. J., Sacchettini, J. C., Sauter, N. K., and Terwilliger, T. C. (2002) PHENIX: building new software for automated crystallographic structure determination, *Acta Crystallogr., D: Biol. Crystallogr. 58*, 1948−1954.
23. Emsley, P., and Cowtan, K. (2004) Coot: model-building tools for molecular graphics, *Acta Crystallogr., D: Biol. Crystallogr. 60*, 2126−2132.
24. Murshudov, G. N., Vagin, A. A., and Dodson, E. J. (1997) Refinement of macromolecular structures by the maximum-likelihood method, *Acta Crystallogr., D: Biol. Crystallogr. 53*, 240−255.
25. CCP4 (1994) The CCP4 suite: programs for protein crystallography, *Acta Crystallogr., D: Biol. Crystallogr. 50*, 760−763.
26. Krissinel, E., and Henrick, K. (2005) Detection of protein assemblies in crystals, *CompLife 3695*, 163−174.
27. Humke, E. W., Shriver, S., Starovasnik, M. A., Fairbrother, W. J., and Dixit, V. M. (2000) ICEBERG: a novel inhibitor of interleukin-1beta generation, *Cell 103*, 99−111.
28. Qin, H., Srinivasula, S., Wu, G., Fernandes-Alnemri, T., Alnemri, E. S., and Shi, Y. (1999) Structural basis of procaspase-9 recruitment by the apoptotic protease-activating factor 1, *Nature 399*, 549−557.
29. Vaughn, D. E., Rodriguez, J., Lazebnik, Y., and Joshua-Tor, L. (1999) Crystal structure of Apaf-1 caspase recruitment domain: an alpha-helical Greek key fold for apoptotic signaling, *J. Mol. Biol. 293*, 439−447.
30. Liu, Y., and Eisenberg, D. (2002) 3D domain swapping: as domains continue to swap, *Protein Sci. 11*, 1285−1299.
31. Inohara, N., Chamaillard, M., McDonald, C., and Nunez, G. (2005) NOD-LRR proteins: role in host-microbial interactions and inflammatory disease, *Annu. Rev. Biochem. 74*, 355−383.
32. Schweizer, A., Briand, C., and Grutter, M. G. (2003) Crystal structure of caspase-2, apical initiator of the intrinsic apoptotic pathway, *J. Biol. Chem. 278*, 42441−42447.
33. Knaus, K. J., Morillas, M., Swietnicki, W., Malone, M., Surewicz, W. K., and Yee, V. C. (2001) Crystal structure of the human prion protein reveals a mechanism for oligomerization, *Nat. Struct. Biol. 8*, 770−774.

BI7016602